THE JOURNAL OF BIOLOGICAL CHEMISTRY VOL. 288, NO. 4, pp. 2157–2166, January 25, 2013

βIII Spectrin Regulates the Structural Integrity and the Secretory Protein Transport of the Golgi Complex*[S]

Received for publication, July 31, 2012, and in revised form, November 28, 2012 Published, JBC Papers in Press, December 11, 2012, DOI 10.1074/jbc.M112.406462

Laia Salcedo-Sicilia[‡1], Susana Granell[‡2], Marko Jovic[§], Adrià Sicart[‡3], Eugenia Mato[‡¶], Ludger Johannes[‖], Tamas Balla[§], and Gustavo Egea[‡ ‡‡4]**

From the [‡]Department de Biologia Cel·lular, Immunologia i Neurociències, Facultat de Medicina, Universitat de Barcelona, 08036 Barcelona, Spain, the [§]Section on Molecular Signal Transduction, Program for Developmental Neuroscience, NICHD, National Institutes of Health, Bethesda, Maryland, the [‖]Institut Curie, Centre de Recherche, Traffic, Signaling, and Delivery group, 26 rue d'Ulm, 75005 Paris, France, **CNRS UMR144, France, the [¶]*Centro de Investigación Biomédica en Red en Bioingeniería, Biomateriales y Nanomedicina, Hospital de la Santa Creu i Sant Pau, 08025 Barcelona, Spain, and the [‡‡]Instituts d'Investigació Biomèdica August Pi i Sunyer i de Nanociència i Nanotecnologia (IN2UB), 08036 Barcelona, Spain*

Background: βIII spectrin function at the Golgi remains unclear.
Results: βIII spectrin is enriched in distal Golgi compartments and supports anterograde transport. PI4P is determinant for the βIII spectrin association with Golgi membranes.
Conclusion: βIII spectrin is necessary for the structural and functional organization of the Golgi.
Significance: We provide new *in vivo* insights of the role of βIII spectrin at the Golgi.

A spectrin-based cytoskeleton is associated with endomembranes, including the Golgi complex and cytoplasmic vesicles, but its role remains poorly understood. Using new generated antibodies to specific peptide sequences of the human βIII spectrin, we here show its distribution in the Golgi complex, where it is enriched in the *trans*-Golgi and *trans*-Golgi network. The use of a drug-inducible enzymatic assay that depletes the Golgi-associated pool of PI4P as well as the expression of PH domains of Golgi proteins that specifically recognize this phosphoinositide both displaced βIII spectrin from the Golgi. However, the interference with actin dynamics using actin toxins did not affect the localization of βIII spectrin to Golgi membranes. Depletion of βIII spectrin using siRNA technology and the microinjection of anti-βIII spectrin antibodies into the cytoplasm lead to the fragmentation of the Golgi. At ultrastructural level, Golgi fragments showed swollen distal Golgi cisternae and vesicular structures. Using a variety of protein transport assays, we show that the endoplasmic reticulum-to-Golgi and post-Golgi protein transports were impaired in βIII spectrin-depleted cells. However, the internalization of the Shiga toxin subunit B to the endoplasmic reticulum was unaffected. We state that βIII spectrin constitutes a major skeletal component of distal Golgi compartments, where it is necessary to maintain its structural integrity and secretory activity, and unlike actin, PI4P appears to be highly relevant for the association of βIII spectrin the Golgi complex.

In erythrocytes and nucleated cells, there is a spectrin-based skeleton that supports cell shape and maintains the organization and stability of the plasma membrane and its mechanical properties (1–3). Spectrin is a cytoskeletal protein that binds simultaneously to integral membrane proteins, cytosolic proteins, and certain phospholipids to create a multifunctional scaffold. Spectrins are composed of α and β subunits, which are assembled side by side to form rod-like αβ dimers, which in turn self-associate to form tetramers. However, β spectrins can also exist as homopolymeric complexes. Although mammalian red blood cells contain only one type of spectrin tetramer (αIβI subunits), nucleated cells contain numerous isoforms of both subunits, which are located in diverse endomembrane systems. The existence of a Golgi-localized, spectrin membrane skeleton was reported almost 20 years ago (4). Similarly to what occurs in erythrocytes and other cell types, such as epithelial cells (5, 6), Golgi-localized spectrin could act as an extensive, two-dimensional interactive platform on the cytoplasmic surface of Golgi cisternae regulating its shape and transport functions (7–9). First evidences of spectrin on Golgi and cytoplasm vesicles were based on the reactivity of erythroid βI spectrin-specific antibodies with a single polypeptide in purified rat liver Golgi membranes with a similar molecular mass to erythroid β spectrin (≈220 kDa), and on the ability of βI spectrin peptides to compete with the function of Golgi spectrin (10, 11). Due to the problems with its precise molecular identification, this band was initially referred to as $\beta I\Sigma^{*}$ spectrin, but after definite identification, it was named βIII spectrin (12). Over the years, specific isoforms of spectrin-binding partners typically present in the plasma membrane of red blood cells have been localized in the Golgi, such as ankyrin (Ank_{G119} and Ank_{195}) (13, 14), protein 4.1 (4.1B) (15), anion exchanger (AE2) (16), and tropomyosin (17).

* This work was supported by a grant BFU2009-07186 (to G. E,) and by the intramural Research Program of the Eunice Kennedy Shriver National Institute of Child Health and Human Development of the National Institutes of Health (to M. J. and T. B.)
[S] This article contains supplemental Figs. S1–S8.
[1] Recipient of a FPI predoctoral fellowship from Ministry of Science and Innovation.
[2] Recipient of a Beatriu de Pinós postdoctoral contract from the Generalitat de Catalunya.
[3] Recipient of a fellowship from the University of Barcelona.
[4] To whom correspondence should be addressed: Facultat de Medicina, Universitat de Barcelona, C/ Casanova 143, 08036 Barcelona, Spain. Tel.: 34-934021909; Fax: 34-934021907; E-mail: gegea@ub.edu.

Disruption of the Golgi by brefeldin A (BFA)[5] quickly releases spectrin from the Golgi, which suggests that its recruitment to Golgi membranes is ADP ribosylation factor-dependent (4, 18). βIII spectrin interacts with $PI(4,5)P_2$ (18–20), and in the absence of its synthesis, βIII spectrin is phosphorylated at Ser and/or Thr residues leading to its partial dissociation from the Golgi and to its fragmentation (21). In respect to protein trafficking, overexpression of the N-terminal five repeats of $\beta I\Sigma^*$ spectrin disrupts Na^+/K^+-ATPase delivery to the plasma membrane (22). Post-Golgi trafficking of glutamate transporter EAAT4 and other synaptic proteins is also impaired when mutations in the βIII spectrin occur in spinocerebellar ataxia type 5 (23–27). β spectrin participates in the dynein-mediated cargo (melanin) and organelle transport (melanosomes) along microtubules (28), and βIII spectrin binds to the dynactin subunit Arp1 *in vitro* (29). In late endosomes, it requires the active action of the tripartite complex Rab7-RILP and ORP1L for their dynein-dependent translocation to the minus-end of microtubules (30).

In the present report, using new polyclonal antibodies generated against different peptides of the human βIII spectrin, we provide new insights into the role of the protein at the Golgi. We found that (i) βIII spectrin is enriched in distal Golgi compartments; (ii) βIII spectrin is necessary to maintain both the perinuclear ribbon-like morphology of the Golgi and the anterograde but not retrograde protein transport; and (iii) PI4P contributes to the association of βIII spectrin with Golgi membranes.

EXPERIMENTAL PROCEDURES

Antibodies and Reagents—Mouse monoclonal antibodies to GM130 and Golgin97 were from Transduction Laboratories (Lexington, KY) and Molecular Probes (Paisley, UK), respectively. Sheep anti-TGN46 and mouse anti-GST were purchased from Abcam (Cambridge, UK), and mouse anti-p190 RhoGAP was from BD Biosciences. Mouse monoclonal antibodies to Myc (clone 9E10) and transferrin receptor, and rabbit polyclonal antibody to RhoGDI and GFP were from Sigma-Aldrich, Invitrogen, Santa Cruz Biotechnology, and Molecular Probes, respectively. Mouse monoclonal antibody to CTR433 was kindly provided by M. Bornens (Institute Curie, Paris, France). Anti-HA antibodies were purchased to Abcam. Antibodies to βI and βII spectrins were from Santa Cruz Biotechnology, respectively, and Novus Biologicals (St. Louis, MO). HEL92.1.7 cell lysates were from Santa Cruz Biotechnology. Cyanine 3-conjugated rabbit secondary antibodies were from Jackson ImmunoResearch Laboratories (West Grove, PA) and Alexa Fluor 488-conjugated anti-mouse, anti-rabbit, and anti-sheep antibodies were obtained from Molecular Probes. Peroxidase-conjugated secondary antibodies were from Promega (Eugene, OR). Protein A-agarose beads from Santa Cruz Biotechnology. Latrunculin B, nocodazole, rapamycin, and mowiol were from Calbiochem (Darmstadt, Germany). Brefeldin A (BFA) was provided by Sigma-Aldrich, and jasplakinolide was from Invitrogen. ^{35}S-Labeled protein labeling mix (^{35}S-EXPRESS) was from PerkinElmer Life Sciences. Endoglycosilase H (Endo H) was purchased from New England Biolabs.

Cell Lines and Cell Culture—Immortalized human pigment epithelial hTERT-RPE1 cells were cultured in DMEM/F12 1:1 (Invitrogen). Normal Rat Kidney, COS-7, and HeLa cells that constitutively express VSV-G-GFP (a gift of V. Malhotra, Centre for Genomic Regulation, Barcelona, Spain) were grown in DMEM, all of them containing 10% of FBS. All culture media were supplemented with 1 mM sodium pyruvate, 2 mM glutamine, 100 units/ml penicillin, and 100 μg/ml streptomycin. Cells were grown in a humidified incubator in 5% CO_2 at 37 °C.

Transfection of Plasmids and siRNAs—Plasmids were transfected with FuGENE® HD (Promega) following the manufacturer's recommendations. Experiments to evaluate the effects of transfection were performed at least 16 h later. siRNAs for human βIII spectrin were purchased from Dharmacon (ON-TARGET*plus* siRNAs; Ref. L-012770-01-0005). siRNAs were employed in two cycles of siRNA treatment (20 nM each) with a delay between them of 24 h, and for a total of 96 h using Hiperfect® as transfection agent (Qiagen, Hilden, Germany). All siRNA-mediated knockdown experiments were validated with a pool of four non-targeting siRNAs (Dharmacon, D-001810-10^{-05}).

Immunofluorescence Microscopy—Cells were fixed in 4% paraformaldehyde in PBS for 10 min, rinsed in PBS, and incubated in PBS containing 50 mM ammonium chloride. Then, cells were permeabilized for 10 min in PBS containing 1% BSA and 0.1% saponin. Primary antibodies were incubated for 1 h and secondary antibodies for 45 min diluted in PBS containing 1% BSA. Working dilutions were as follows: anti-βIII spectrin (1:150); anti-GM130 (1:1000); anti-CTR433 (1:5); anti-Golgin97 (1:300); anti-TGN46 (1:500); anti-GST (1:200); anti-Myc (1:200); Cy3-anti-rabbit (1:250), and Alexa Fluor 488 anti-mouse, anti-rabbit, or anti-sheep (1:500). Immunostained coverslips were mounted on microscope slides using mowiol. Microscopy and imaging were performed either with an Olympus BX60 epifluorescence microscope with a cooled Orca-ER CCD camera (Hamamatsu Photonics, Japan) or with a Leica TCS-SL confocal microscope (Leica Microsystems Heidelberg, Manheim, Germany). The images were processed using Image J software and Adobe Photoshop CS (Adobe Systems, San Jose, CA). The analysis of the compactness of the Golgi was carried out as described (31).

Subcellular Fractionation—A pellet of RPE1 cells was resuspended in XB buffer (20 mM Hepes, 150 mM KCl, pH 7.7) supplemented with protease inhibitor mixture (Sigma-Aldrich), five times the volume of the pellet. Extracts were mechanically cracked with an insulin syringe and centrifuged at 1,000 × *g* for 10 min to remove cell debris and nuclei. The supernatant (total fraction) was subsequently subjected to a 60-min ultracentrifugation at 60,000 rpm using a MLA-130 rotor (Beckman Coulter Inc., Brea, CA). The resulting supernatant was the cytosolic fraction, whereas the membrane pellet was solubilized in the same volume as the cytosolic fraction in radioimmune precipitation assay buffer (50 mM Tris-HCl, pH 7.4, 150 mM NaCl, 1% Triton X-100, 1% sodium deoxycholate, 0.1% SDS, 1 mM EDTA plus protease inhibitors) for 60 min at 4 °C. The mem-

[5] The abbreviations used are: BFA, brefeldin A; TGN, *trans*-Golgi network; ER, endoplasmatic reticulum; $PI(4,5)P_2$; phosphatidylinositol 4,5-biphosphate; PI4P, phosphatidylinositol 4-phosphate; PH, pleckstrin homology; Endo H, endoglycosilase H; ABD, actin-binding domain; OSBP, oxysterol-binding protein; FAPP1, four-phosphate adaptor protein 1.

brane fraction was then recentrifuged for 60 min at 60,000 rpm to remove insoluble material. All subcellular fractions were subjected to 6% or 10% (v/v) SDS-polyacrylamide gel electrophoresis. We used βIII spectrin antibodies (1:500) to detect the βIII spectrin, anti-RhoGDI antibodies (1:1000) as a cytosolic marker, and anti-transferrin receptor antibodies (1:5000) as a membrane marker. Golgi-enriched fractions from rat liver were prepared as described previously (32).

Immunoprecipitation and Western Blot Experiments—Whole cell extracts were prepared by adding 300 μl of modified radioimmune precipitation assay buffer containing protein (aprotinin, leupeptin, and pepstatin A) and phosphatase (sodium orthovanadate and phenylmethylsulfonyl fluoride) inhibitors. Samples were incubated for 10 min on ice and then gently sonicated (two rounds of 5 s per sample) and centrifuged (1,000 × *g* for 10 min at 4 °C). Equal amounts of sample lysates (500 μg) were incubated overnight with the respective antibody (5 μg of anti-HA or anti-βII spectrin antibodies) and with 50 μl of 50% slurry of protein A-Sepharose beads. The next day, beads were rinsed three times in TA buffer (20 mM Tris-HCl, pH 7.5, 5 mM sodium azide, 1 mM PMSF, 1 mM EGTA). Proteins were eluted from Sepharose beads by adding 20 μl of loading buffer 5× (containing 10% β-mercaptoethanol). Subsequently, samples were processed for Western blotting.

Protein Transport Assays—To examine the VSV-G protein transport, stable HeLa cells that constitutively express VSV-G-GFP were grown on 35-mm dishes, transfected with the respective pools of siRNAs, and incubated at 37 °C for 72 h. The cells were then incubated at 40 °C for 16 or 24 h. Cycloheximide was added to a final concentration of 100 μg/ml (on the last 30 min), and then the cells were shifted to 32 °C to allow transport. At the indicated times, cells were fixed and processed for immunofluorescence analysis. In addition, the cells were solubilized with 0.5% SDS and 1% 2-mercaptoethanol (0.1 ml/dish) and heated at 100 °C for 10 min. A portion of lysate was digested with Endo H following the manufacturer's protocol and then subjected to SDS-PAGE on 8% gels. VSV-G-GFP was visualized by immunoblotting with a polyclonal anti-GFP (1:25,000) antibody, and intensities of the immunostained bands were quantified.

For the protein secretion experiments, RPE1 cells transfected with siRNA non-targeting, siRNA βIII spectrin, or treated with BFA (acting as a positive control) were starved for 30 min in Met/Cys-free medium and then pulse-labeled with 20 μCi of [^{35}S]-Met/Cys mix per well in a six-well plate for 10 min. Then, cells were rinsed with cold complete media and transferred to 19 °C for 3h to let the accumulation of ^{35}S-labeled proteins synthesized *de novo*. After the incubation, cells were washed twice with 5% BSA in PBS and then shifted to 37 °C. To determine the kinetics of secretion, culture supernatants were collected at different times. ^{35}S-Labeled secreted proteins were precipitated with 20% trichloroacetic acid (TCA), washed with cold acetone, and quantified by scintillation counting. To determine total incorporation of [^{35}S]Met/Cys into cellular proteins, cells were lysed with 0.1 N sodium hydroxide in 0.1% sodium deoxycholate, treated with TCA, and processed as above. For additional control, cells remained on ice before supernatants were collected.

To follow the retrograde transport of Shiga toxin (STxB), RPE1 cells treated with siRNA non-targeting or siRNA βIII spectrin were starved for 30 min in medium without FBS and then incubated with 0.5 μg/ml of cyanine 3-tagged STxB-KDEL for 1 h at 4 °C, washed with cold PBS to remove the unbound toxin, and transferred to 37 °C for indicated times. Cells were then processed by indirect immunofluorescence.

Microinjection Experiments—NRK cells were plated onto 25-mm diameter poly-D-lysine-coated coverslips 1 day before the microinjection. Purifed IgG fractions of anti-βIII spectrin antibody 33 or preimmune serum together with dextran red were co-microinjected into the cell cytoplasm with an automated microinjection system (Leica AS TP). After microinjection, the coverslips were transferred to a Petri dish containing fresh culture medium and returned to the incubator. After 5 h, cells were fixed, and the Golgi was immunostained as indicated above.

Plasmids—Plasmids encoding GST-PH-FAPP1 and GFP-PH-OSBP were provided by M. A. de Matteis (Univeristy of Naples, Naples, Italy) and T. Levine (University College London, London, UK), respectively. Untagged and Myc-tagged human βIII spectrin plasmids were kindly provided by L. Ranum (University of Minnesota). Plasmids to rat Myc-tagged βII spectrin and to human HA-tagged βII spectrin were provided, respectively, by M. Jackson (University of Edimburg, UK) and by Addgene (plasmid 31070 kindly provided by V. Bennett). The PH domain of βIII spectrin was amplified from the untagged βIII spectrin plasmid with the forward and reverse primers as follows: 5′-TTTGAATTCTCCACCATCCACACAAGCACCC-3′ and 5′-TTTGGATCCCTACTTGTTCTTCTTAAAGAAGCT-3′. Then, the PCR product was subcloned into the pEGFP-C1 vector after cutting with EcoRI and BamHI restriction enzymes. The actin-binding domain (ABD) of βIII spectrin was generated from the untagged βIII spectrin construct using the following forward and reverse primer pairs: 5′-AGCTGAATTCACCACCATGAGCAGCACG CTGTCACCC-3′ and 5′-AGCTGGTACCCAGCTCCGAAGGCCAGGGACTC-3′. This piece was then inserted between the EcoRI-KpnI sites of the pEGFP-N3 vector. Human mRFP-FKBP12-Sac1, mRFP-FKBP12 only, and TGN38-FRB-CFP have been used as described previously (33).

βIII Spectrin Antibody Preparation—A first round of anti-βIII spectrin antibodies was produced at the University Pompeu Fabra (Barcelona, Spain). Briefly, peptides 3 and 5 were synthesized, conjugated to a keyhole limpet hemocyanin and used to immunize rabbits to produce antibodies 33 to 38 (see Fig. 1*A*). Final bleedings were purified by affinity chromatography with the respective peptides. A second round of anti-βIII spectrin antibodies was produced by Eurogentec (Liège, Belgium) using peptides 1, 2, and 4, which were also conjugated to keyhole limpet hemocyanin and injected to immunize rabbits. Final bleedings were also affinity purified.

RESULTS

βIII Spectrin Is Enriched in Distal Golgi Compartments—We generated a set of new rabbit polyclonal antibodies from synthesized peptides corresponding to different regions of βIII spectrin (Fig. 1*A*). For each antiserum, the corresponding IgG fraction and high-affinity purified antibodies were tested for

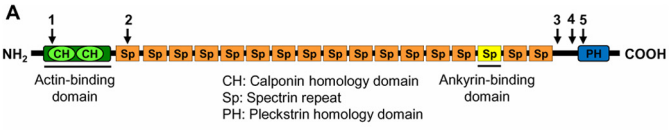

Peptide number	Amino acid sequence and position	Antibody number
1	YSDINNRWDLPDSDWDN (20-35 aa)	82 and 83
2	LRANNQKVYTPREGR (376-390 aa)	86 and 87
3	TALEEREKERKRKREE (2076-2091 aa)	36, 37 and 38
4	EGPGPGSGDEANGPRGER (2165-2182 aa) (Stankewich et al., 1998)	84 and 85
5	CRKQEMEAFGKKAANRS (2226-2242 aa)	33, 34 and 35

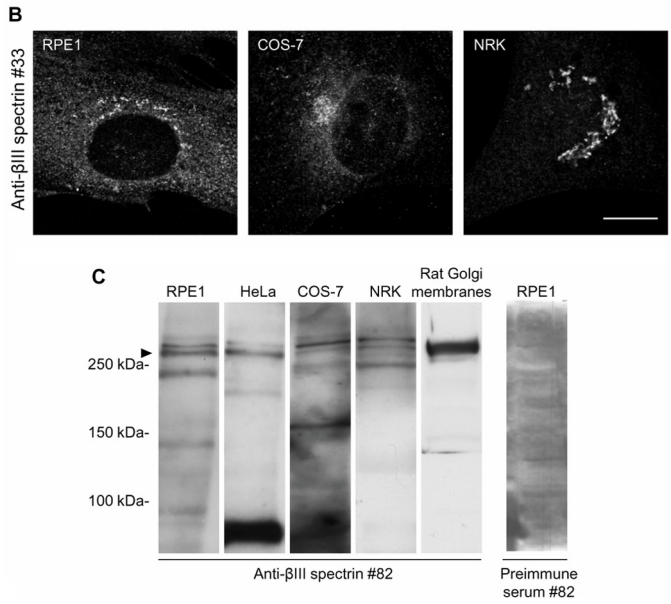

FIGURE 1. **Characterization of antibodies against specific peptide sequences of human βIII spectrin.** *A*, schematic representation of human βIII spectrin and targeted regions are indicated by *arrows*. Peptide 1 targets the ABD; peptide 2 targets the first spectrin repeat (*Sp*); peptides 3 and 4 target the nonspecific region; and peptide 5 targets the PH domain. The table shows the complete amino acid sequence of the five selected peptides. The names of obtained antibodies are also given. *B*, immunostaining of RPE1, COS-7, and NRK cells employing antibody 33. The images were analyzed by confocal microscopy. *Bar*, 10 μm. *C*, Western blotting analysis using preimmune serum or affinity purified antibody 82 of whole cell lysates from indicated cell types and Golgi-enriched fractions from rat liver. *Arrowhead* indicates the expected βIII spectrin band.

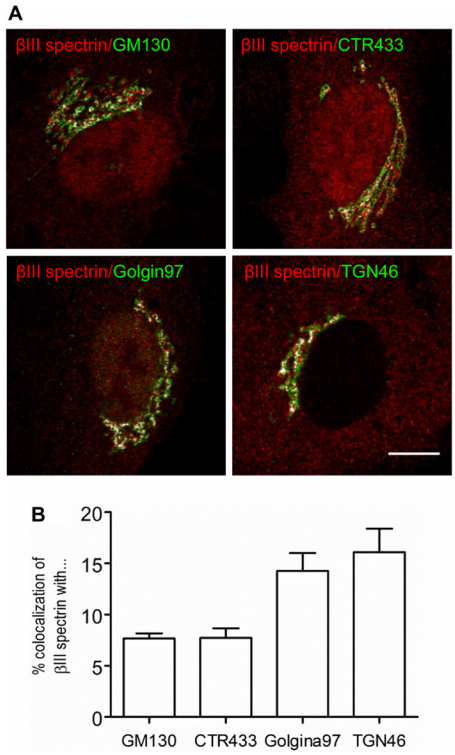

FIGURE 2. **βIII spectrin is enriched in distal Golgi compartments.** *A*, co-localization of βIII spectrin with Golgi markers. RPE1 cells were co-stained with anti-βIII spectrin antibody 33 and antibodies against *cis*- (GM130), medial- (CTR433), *trans*-Golgi (Golgin97), or the TGN (TGN46) proteins. Merge pixels are shown in *white* to facilitate the visualization of the co-labeling. *Bar*, 10 μm. *B*, quantitative analysis of the co-localization shown in *A*.

their ability to stain the Golgi by indirect immunofluorescence and/or by Western blotting to recognize a band with the expected molecular weight of the protein (≈270 kDa). By indirect immunofluorescence, antibody 33 stained a peri- or juxtanuclear nuclear compartment corresponding to the Golgi complex in several clonal cell lines (Figs. 1*B* and 2). Antibody 82 recognized by Western blotting an immunoreactive double band > 250 kDa in a variety of whole cell lysates and in Golgi-enriched fractions from rat liver (Fig. 1*C*). However, after knocking down βIII spectrin expression by RNAi, only the lower band of the doublet was affected (see Fig. 3*A* and supplemental Fig. S1*A*). Moreover, antibody 82 recognized the exogenously expressed Myc-tagged βIII spectrin in RPE1 cells (supplemental Fig. S1*A*) but not βI or βII spectrins (supplemental Fig. S1, *B–D*). The rest of the antibodies were much less efficient, and therefore, we chose antibodies 33 and 82 for immunofluorescence and Western blotting experiments, respectively. To examine in more detail the subcellular distribution of βIII spectrin in the Golgi, we performed co-localization studies using confocal microscopy with well established markers of the proximal (GM130 and CTR433) and distal (Golgin97 and TGN46) Golgi compartments (Fig. 2). In RPE1 cells, βIII spectrin distribution overlapped with all of the Golgi markers tested (Fig. 2*A*), but the co-localization was much tighter with the *trans*-Golgi and TGN markers (Fig. 2*B*). Furthermore, we always observed persistent cytoplasmic and nuclear (excluding nucleoli) stainings (Fig. 3*B*), the presence and intensity of which was variable depending on the cell examined.

βIII Spectrin Is Necessary for the Structural Integrity of the Golgi—To determine the contribution of βIII spectrin to the structural organization of the Golgi, we imaged RPE1 cells following βIII spectrin depletion using siRNA technology (Fig. 3). Cells transfected for a total of 96 h with a pool of four siRNAs against human βIII spectrin exhibited a significant reduction in βIII spectrin protein level (up to 85%) (Fig. 3*A*). Note that the use of individualized siRNA did not improve the level of protein reduction and therefore, we chose the pool of siRNAs (Fig. 3*A*, *lane 2*) for subsequent knockdown experiments. In knockdown cells, βIII spectrin was not observed at the Golgi. Concomitantly to the absence of βIII spectrin, knocked down cells showed a fragmented Golgi (Fig. 3*B*), which was quantified using an index of "compactness" calculated from measurements of the area and perimeter of each Golgi element (31). Results showed that the Golgi in βIII spectrin-depleted cells is significantly less compact than in non-silenced cells (Fig. 3*C*). A fragmented Golgi phenotype was also observed in cells micro-

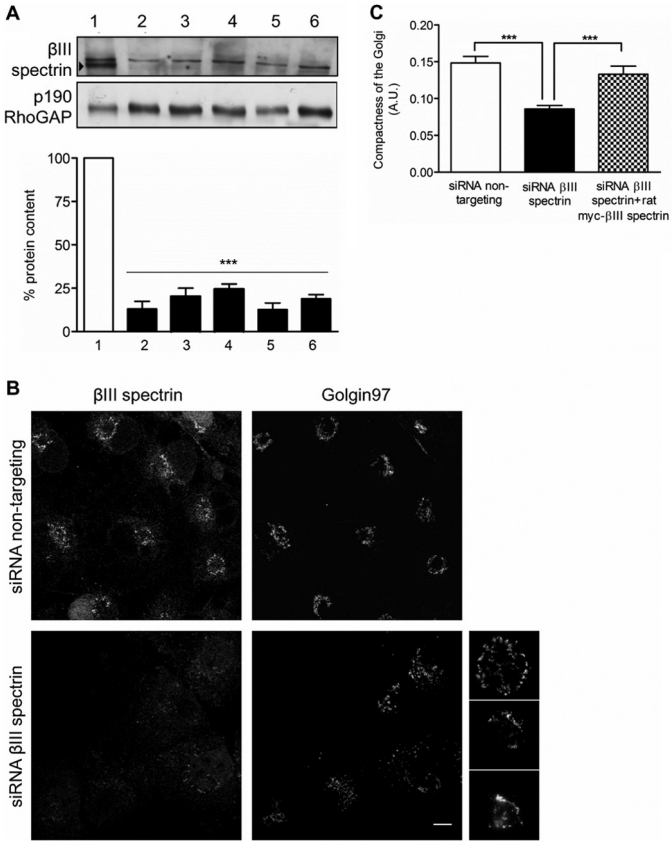

FIGURE 3. **Depletion of βIII spectrin fragments the Golgi.** (A). Silencing of βIII spectrin in RPE1 cells. Total cell lysate from RPE1 cells transfected for 96 h with control siRNA (non-targeting siRNA pool; *lane 1*) or βIII spectrin siRNA pool composed of four siRNAs (*lane 2*) or individualized siRNA (from 1 to 4; *lanes 3–6*, respectively) were subjected to immunoblot analysis using affinity-purified antibodies against βIII spectrin. Note the reduction of the lower electrophoretic band indicated with the *arrowhead*. Values are the mean ± S.E. from three independent experiments. Statistical significance according to one-way analysis of variance, using Bonferroni's multiple comparison test (***, $p \leq 0.001$ in contrast to siRNA non-targeting). p190 RhoGAP was used as a loading control. *B*, fragmentation of the Golgi in βIII spectrin-depleted RPE1 cells. Cells transfected with control siRNA or βIII spectrin siRNA pool were stained with anti-βIII spectrin antibodies and the *trans*-Golgi marker Golgin97. Note the fragmented and variably dispersed Golgi phenotypes observed in βIII spectrin-depleted cells (*asterisks*). *Bar*, 10 μm. *C*, quantitative analysis of the fragmentation of the Golgi in control, βIII spectrin-depleted cells shown in *B*, and in knockdown cells expressing rat Myc-tagged βIII spectrin. The data show the mean ± S.E. from three independent experiments. Statistical significance according to one-way analysis of variance using Bonferroni's multiple comparison test; ***, $p \leq 0.001$.

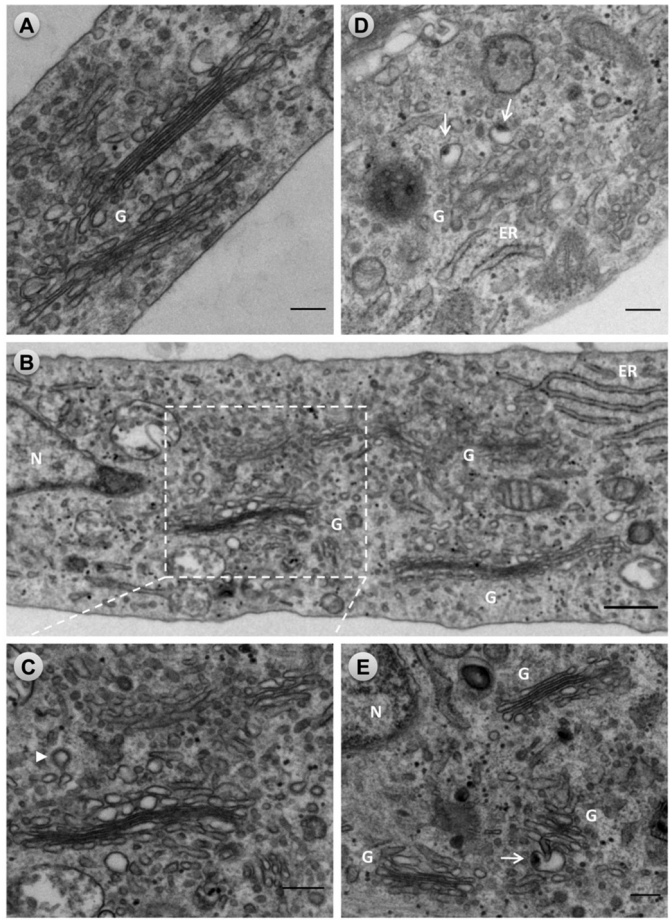

FIGURE 4. **Ultrastructural alterations of the Golgi complex in βIII spectrin-silenced cells.** RPE1 cells transfected with siRNA non-targeting (control) or βIII spectrin siRNA pools for 96 h were fixed and processed for conventional transmission electron microscopy. *A*, characteristic ultrastructure of the Golgi showing flat and attached cisternae in a control cell. *B*, panoramic area of the Golgi region in a knockdown cell showing Golgi stacks with variable ultrastructural alterations. One of these Golgi stacks is enlarged in *C*, in which distal cisternae are swollen. The *arrowhead* indicates the presence of a clathrin-coated vesicle. *D* and *E*, examples of Golgi fragments seen in silenced cells. Note the presence of distal swollen cisternae and/or tubulovesicular structures containing a large electrondense material (*arrows*). In some of these Golgi fragments, cisternae are not completely flat but remain attached (*E*). Box indicated in panel *B* is enlarged in panel *C*. *Bars*, 200 nm. *G*, Golgi complex: *N*, nucleus.

injected with purified anti-βIII spectrin IgG fraction or affinity purified antibodies into their cytoplasm (supplemental Fig. S2). When knockdown cells were examined under the electron microscope (Fig. 4), many Golgi stacks of different size were dispersed around the nucleus (Fig. 4, *B–E*). The ultrastructural impairments of Golgi fragments were variable in some extent (most likely reflecting the variable degree of silencing of βIII spectrin in cells), but consistently, we observed the swelling of distal Golgi compartments (Fig. 4, *B* and *C*), identified by the close presence of clathrin-coated vesicles (Fig. 4*C*, *arrowhead*). In many cases, swollen structures contained an electrondense internal core (Fig. 4, *D* and *E*, *arrows*). In some Golgi fragments, cisternae showed a tortuous shape, the lumen of which was not always clearly visualized in contrast to occur in normal Golgi stacks (compare Fig. 4, *B–D*, with Fig. 4*A*). In contrast, ER cisternae remained unaltered.

βIII Spectrin Participates in the Secretory but Not the Retrograde Protein Transport—We next investigated whether the depletion of βIII spectrin and the resultant Golgi fragmentation have impact on the secretory membrane trafficking. We first examined the anterograde (ER to Golgi) and retrograde (Golgi to ER) membrane flux at the ER-Golgi interface using BFA. Whereas the addition of BFA produced the rapid redistribution of βIII spectrin from the Golgi to the cytoplasm (4), no delay in the disassembly of the Golgi and subsequent merging with the ER was observed (supplemental Fig. S3). However, when the anterograde membrane flux was examined after the BFA washout, the reassembly of the Golgi was blocked in βIII spectrin-silenced cells (Fig. 5, *A* and *B*). We also examined the dynamic disassembly and reassembly of the Golgi in cells treated and subsequently washed out with nocodazole. No difference in the

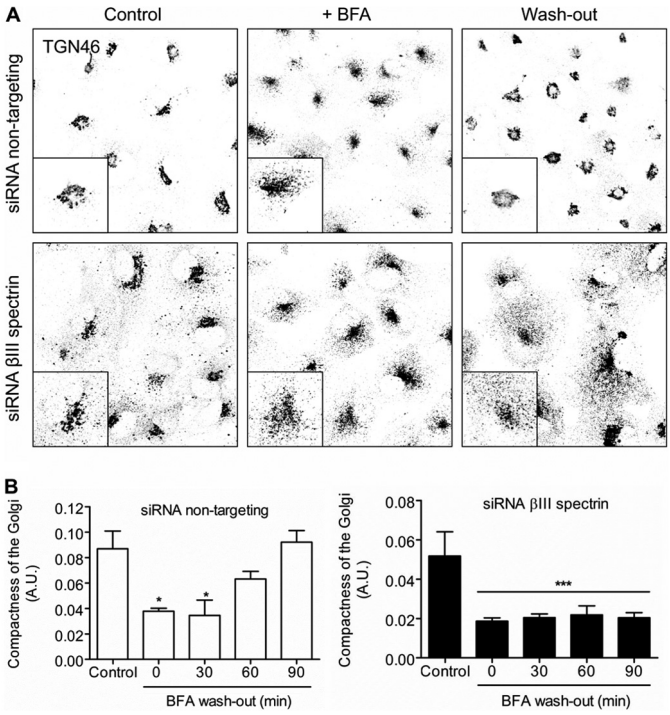

FIGURE 5. **Depletion of βIII spectrin blocks the reassembly of the Golgi.** Cells transfected with control or βIII spectrin siRNA pools were first treated with BFA (2.5 μg/ml for 90 min; +BFA). Thereafter, cells were washed out, fixed at different time points, and co-stained with antibodies to βIII spectrin (not shown) and to TGN46. *Insets* are representative images of enlarged cells. *Bar*, 10 μm. *B*, analysis of the Golgi compactness index in control (siRNA non-targeting) (*left panel*) and βIII spectrin knockdown cells (*right panel*) at different times after BFA wash-out. Values are the mean ± S.E. from three independent experiments (100 cells each). Statistical significance according to one-way analysis of variance using Bonferroni's multiple comparison test (*, $p \leq 0.05$; ***, $p \leq 0.001$). *A.U.*, arbitrary units.

kinetics of Golgi fragmentation after nocodazole treatment was observed between control and silenced cells (supplemental Fig. S3). However, after the wash-out of nocodazole, the Golgi remained largely fragmented in knocked down cells, whereas the Golgi was normally reformed in control cells (supplemental Fig. 4). These results are indicative that the anterograde but not the retrograde membrane trafficking between the ER and the Golgi is impaired by the absence of βIII spectrin.

To explore these alterations in more detail, we monitored the trafficking of cargo such as membrane VSV-G and soluble proteins for the anterograde transport (ER to Golgi/plasma membrane) and the Shiga toxin subunit B for the retrograde transport (plasma membrane to Golgi to ER). We first investigated whether depletion of βIII spectrin interferes with VSV-G transport (Fig. 6). HeLa cells constitutively expressing VSV-G-GFP were transfected for 96 h with non-targeting or βIII spectrin pool of siRNAs. The transfected cells were incubated at 40 °C to accumulate VSV-G in the ER. After the shift to permissive temperature (32 °C), the VSV-G exits from the ER and travels to the plasma membrane passing through the Golgi (Fig. 6*A*). The arrival of VSV-G to the plasma membrane in knocked down cells was slower than in control cells (Fig. 6, *B* and *C*). The analysis of the kinetics of the acquisition of Endo H resistance showed that the delivery of VSV-G from the ER to the Golgi was significantly delayed in βIII spectrin-depleted cells (Fig. 6*D*). We next examined whether the depletion of βIII spectrin equally affected the secretion of ^{35}S-labeled proteins from the Golgi. RPE1 cells were transfected with non-targeting or βIII spectrin targeting siRNA pools. As additional controls, cells were treated previously with BFA or incubated at 4 °C. We observed that βIII spectrin-depleted cells showed a 2-fold reduction in the secretion of labeled proteins (Fig. 6*E*).

The impact of βIII spectrin on retrograde transport of the subunit B of the Shiga toxin that contains in its carboxyl terminus the ER retention sequence KDEL (STxB-KDEL) was also investigated (supplemental Fig. S5). Briefly, control and βIII spectrin-depleted RPE1 cells were incubated with STxB-KDEL at 4 °C for 1 h, rinsed, and then shifted to 37 °C to allow its internalization until the ER with transit in early endosomes and the Golgi (33). No difference in the appearance of the STxB-KDEL to the Golgi and to the ER was observed between control and βIII spectrin-silenced cells.

To assess the specificity of the Golgi structural and transport alterations after the depletion of βIII spectrin, we performed siRNA rescue experiments. To this aim, silenced RPE-1 cells were transfected with a plasmid expressing rat Myc-tagged βIII spectrin. We observed that (i) the protein levels of βIII spectrin were restored (supplemental Fig. 6*A*); (ii) the Golgi fragmentation measured by the Golgi compactness index (Fig. 3*C*), and (iii) the blockade of the Golgi reassembly after the BFA wash-out were both reversed (supplemental Fig. 6*B*).

PI4P but Not Actin Contributes to the Association of βIII Spectrin to the Golgi—It has been previously reported that the ABD and the membrane-associated domain MAD1 target βIΣ* spectrin to the Golgi in MDCK cells (22). In contrast, the dynactin subunit Arp1 binds *in vitro* more efficiently than actin to βIII spectrin (29). Thus, we next investigated to what extent phosphoinositides and actin dynamics contribute to the localization of βIII spectrin to the Golgi *in vivo*. It has been previously reported *in vitro* that the PH domain of β spectrin binds to $PI(4,5)P_2$ with low affinity and poor specificity (35–37). Whereas previous works have shown that $PI(4,5)P_2$ levels mediate *in vitro* the association of βIII spectrin with Golgi membranes and liposomes (18, 20), it is also well known that the intrinsic level of $PI(4,5)P_2$ in the Golgi is very low (38). Therefore, the PH domain of βIII spectrin either has little or no relevance *in vivo* or, alternatively, other phosphoinositide(s) significantly contribute to βIII spectrin recruitment to Golgi membranes. Because PI4P is highly enriched in Golgi membranes (38, 39), we investigated its potential contribution to the association of βIII spectrin to Golgi membranes. For this purpose, the Golgi-associated pool of PI4P was depleted by the rapamycin-induced targeting of a recruitable Sac1 phosphatase to the Golgi (33). COS-7 cells were co-transfected with the Golgi-targeted CFP-TGN38-FRB and the cytosolic mRFP-FKBP12 or the cytosolic mRFP-FKB12-Sac1 phosphatase, whose action onto the Golgi-associated PI4P pool was monitored by the GFP-fused PH domain of OSH1. Cells were fixed and incubated with βIII spectrin antibodies after incubation with rapamycin. We observed a loss of βIII spectrin staining in cells where the Sac1 phosphatase was recruited to the Golgi (Fig. 7, *A* and *B*). Recruitment of FKBP12 without the Sac1 phosphatase was used as a control. Although this negative control also showed some effect in a few cells, its much smaller

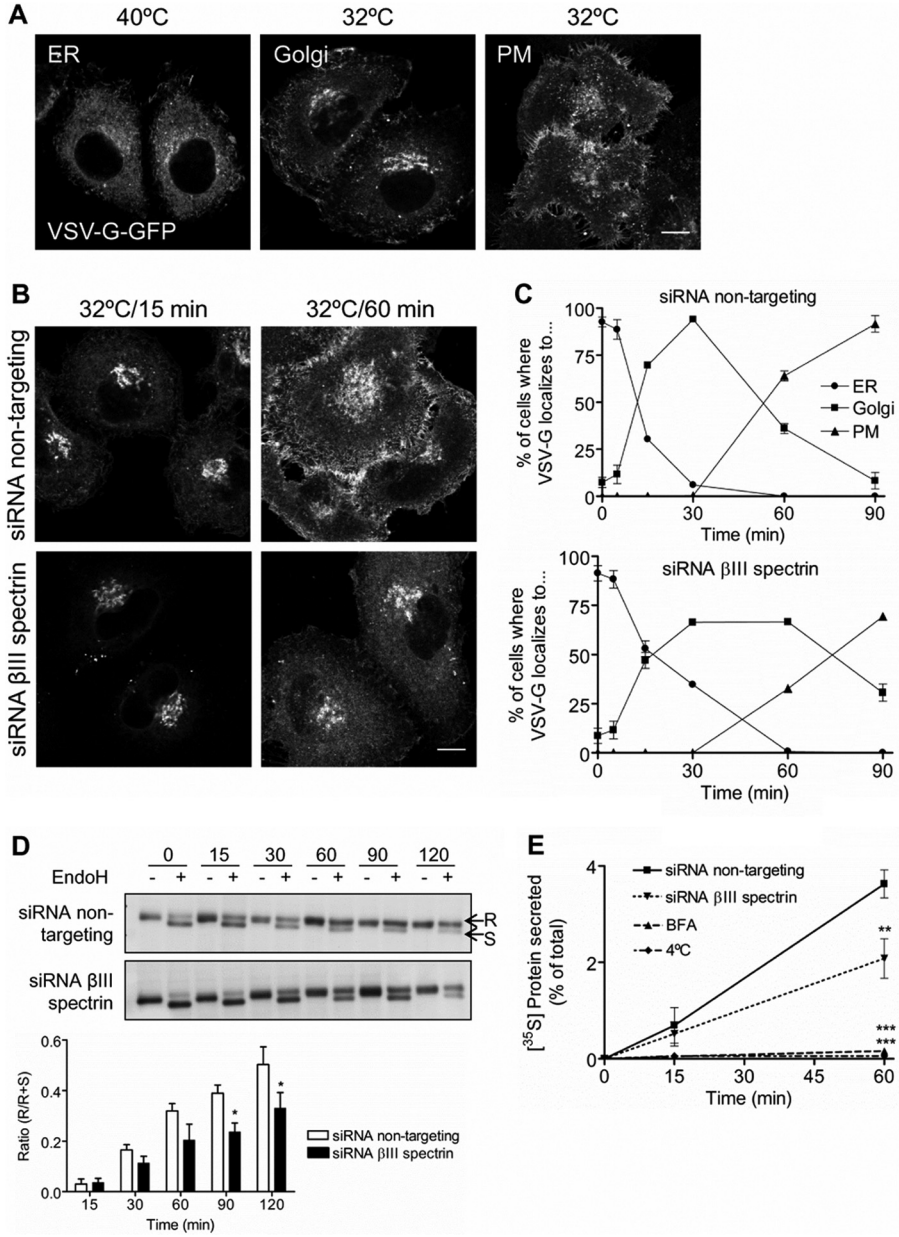

FIGURE 6. **Depletion of βIII spectrin impairs the anterograde transport of the VSV-G and the post-Golgi secretion of ^{35}S-labeled proteins.** *A*, representative images of HeLa cells constitutively expressing VSV-G-GFP mutant form ts045 show the viral protein in the ER at 40 °C, or in the Golgi (30 min) or the plasma membrane (*PM*; 90 min) when cells were shifted to 32 °C. *Bar*, 10 μm. *B*, representative images of VSV-G-GFP expressing HeLa cells silenced with non-targeting or βIII spectrin siRNAs after 15 and 60 min after being shifted to 32 °C. *C*, quantitative analysis of results partially shown in *B*. The graph shows the percentage of the cells in which VSV-G-GFP is mainly visualized to the ER, to the Golgi, or to the plasma membrane. Data are shown as the mean ± S.E. of three independent experiments (100 cells each). *D*, biochemical transport assay for VSV-G-GFP using Endo H. HeLa cells constitutively expressing VSV-G-GFP were transfected for 96 h with siRNA control or against βIII spectrin and incubated at 40 °C for the last 24 h. Then, cells were shifted at 32 °C to induce the transport of VSV-G from the ER, lysed at indicated times, and subjected to Endo H treatment. *R* and *S* indicate Endo H-resistant and -sensitive forms, respectively. The ratio of the amount of Endo H-resistant form to that of total amount is plotted. Values are represented as the mean ± S.E. of three independent experiments. Statistical significance is shown, according to two-way analysis of variance using Bonferroni's post-tests (*, $p \leq 0.05$). *E*, RPE1 cells were transfected with control or with βIII spectrin siRNA. Ninety-six h after the transfection, cells were pulse labeled with [^{35}S]Met/Cys, incubated at 19 °C for 3 h and then shifted to 37 °C. At the indicated times, proteins in the culture supernatants and the cell lysates were precipitated and quantified by scintillation counting. As additional controls, the secretion assay was performed at 4 °C or in cells treated with BFA. Results are the mean ± S.E. from at least three independent experiments. Statistical significance according to two-way analysis of variance using Bonferroni's post-tests (**, $p \leq 0.01$ and ***, $p \leq 0.001$).

effect was attributable to the expression of the TGN38 recruiter construct. Therefore, special attention was paid to compare cells where the TGN38 recruiter was not expressed at high level. As a complementary approach, we also examined whether the PH domain of proteins that are recruited to the Golgi through binding to PI4P were able to displace βIII spectrin from the Golgi (Fig. 7*C*) (40). The PH domains of oxysterol-binding protein (OSBP) and the four-phosphate adaptor protein 1 (FAPP1) have been shown to recognize PI4P (41). It has to be noted that Golgi recruitment of these PH domains is Arf1-dependent, and at high expression levels, they can also sequester Arf1 to induce Golgi fragmentation and interfere with Golgi trafficking via this mechanism (42). Nevertheless, RPE1 cells expressing the GST-tagged PH domain of FAPP1 or the

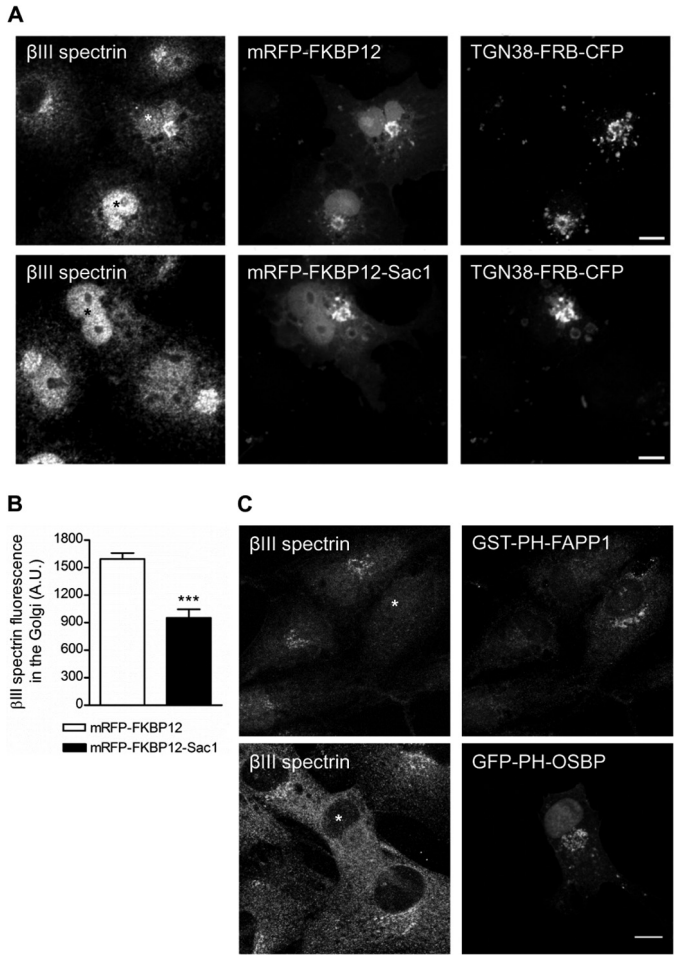

FIGURE 7. **The association of βIII spectrin to Golgi membranes requires PI4P.** *A*, COS-7 cells were transfected with the Golgi-targeted TGN38-FRB-CFP and the cytosolic mRFP12-FKBP only or with the cytosolic mRFP-FKBP12-Sac1 phosphatase. Live cells were preincubated for 5 min with rapamycin (100 nM), fixed, and incubated with antibodies against βIII spectrin. *Bar*, 10 μm. *B*, quantitative analysis of results shown in *A*. Results are the mean ± S.E. from three independent experiments using the Student's *t* test (***, $p \leq 0.001$). *C*, RPE1 cells either expressing the GST-tagged PH domain of FAPP1 or the GFP-tagged PH domain of OSBP were fixed and stained with anti-GST and anti-βIII spectrin antibodies or only with anti-βIII spectrin antibodies, respectively. Note that cells with the Golgi-recruited PI4P Sac1 phophatase or with the presence of the PH domain of either FAPP1 or OSBP in the Golgi showed no staining for βIII spectrin (*asterisks*). *Bar*, 10 μm. *A.U.*, arbitrary units.

GFP-PH domain of OSBP at moderate levels did effectively displace βIII spectrin from the Golgi (Fig. 7*C*). Next, the isolated PH domain of βIII spectrin was cloned into a eukaryotic expression vector tagged with GFP. Strikingly, when this construct was expressed in RPE1 cells, the GFP fluorescence was localized only to the plasma membrane (supplemental Fig. S7*A*). This result indicated that the lipid binding by the βIII spectrin PH domain alone is not sufficient for Golgi localization and has to cooperate with other interactions to drive multivalent Golgi membrane association of the full βIII spectrin molecule. In this respect, we reasoned that the ABD could be one of them. Thus, we cloned and GFP-tagged the isolated ABD of βIII spectrin, and it was subsequently expressed in RPE1 cells. As with the PH domain, the ABD-GFP only localized to the plasma membrane (supplemental Fig. S7*B*). Next, we examined the contribution of actin dynamics in the localization of βIII spectrin to the Golgi. Thus, RPE1 cells were treated with actin drugs that either depolymerize (latrunculin) or stabilize (jasplakinolide) actin filaments and subsequently co-stained for GM130 and βIII spectrin (supplemental Fig. S8*A*). Confocal analysis of immunofluorescence images showed that the compact Golgi was invariably stained for βIII spectrin with no significant changes in response to treatment with either drug. This observation was confirmed when the cytosolic and membrane-associated pools of βIII spectrin were examined by cell fractionation and Western blotting analysis (supplemental Fig. S8, *B* and *C*).

DISCUSSION

Studies from several laboratories, including our own, have implicated actin filaments, actin binding and regulatory proteins, actin motors, and spectrin-based cytoskeleton isoforms in maintaining the structure and protein transport of the Golgi complex in mammalian cells. Whereas the importance of a non-erythroid spectrin-based cytoskeleton at the Golgi in mammalian cells preceded the evidence concerning the involvement of actin-binding and regulatory proteins and myosins, new insights to define the role of spectrin in the Golgi and in the secretory pathway was lagging due, at least in part, to the limited availability of specific molecular tools. Here, we provide new insights in the role of spectrin-based cytoskeleton at the Golgi using new antibodies raised against specific peptide sequences of human βIII spectrin and the siRNA technology to knock down the expression of the protein. We show that PI4P is necessary for the binding of βIII spectrin to the Golgi and that βIII spectrin is important for the maintenance of normal Golgi morphology and for anterograde transport of both membrane and soluble proteins.

In regard to the subcellular localization of βIII spectrin at the Golgi, we found that (i) βIII spectrin is enriched in distal Golgi compartments (see below), and (ii) the staining pattern observed under the confocal microscopy does not show a continuity, but a punctated and dashed pattern that variably matches the Golgi compartment. We do not know what might be the significance of this observation, but we speculate that it might represent the staining of some of the two regions that defines the Golgi stack: the central, compact or poorly fenestrated, or the lateral, non-compact, or highly fenestrated (43). The former would be analogous to what occurs in red blood cells whose submembraneous localization determines their characteristic discoid shape; conversely, the latter would be consistent with the previously postulated role of β spectrin as an exocytic coat protein (9). Ultrastructural localization of βIII spectrin at the Golgi should definitively resolve this possibility but, unfortunately, none of our antibodies were suitable for immunoelectron microscopy techniques.

The co-localization of βIII spectrin was the highest with markers of the distal Golgi compartments. A gradient of PI4P enrichment across the Golgi stack has been postulated with *cis*-Golgi harboring the least amount of PI4P and the TGN the greatest (44, 45). Given the importance of PI4P for the association of βIII spectrin to the Golgi, the enrichment of βIII spectrin to distal Golgi could also follow this PI4P gradient. Conversely, βIII spectrin could actively participate in the membrane organization of cisternae by regulating the spatial avail-

ability of the pool of PI4P, which is used as substrate in the local lipid homeostasis, and/or as a lipid recruiter of PI4P-binding proteins involved both in transport carrier biogenesis (cargo sorting, packaging and trafficking) and lipid homeostasis such as OSBP1, FAPP2, CERT, or GOLPH3 (45–47). The potential regulation of βIII spectrin on the PI4P availability could also explain the observation that secretory transport carriers contain less PI4P than do the TGN membranes from which they are budded (48).

βIII spectrin participates in the maintenance of the characteristic morphology of the Golgi complex because depletion of the protein by siRNAs leads to the fragmentation of the organelle. Ultrastructural results indicate that βIII spectrin participates in the maintenance of the characteristic flattened morphology of cisternae, particularly in those of distal compartments. The presence of an electrondense material core in the lumen of swollen elements in knockdown cells results most likely from the accumulation of luminal cargo in the TGN.

Previously it was postulated that the fragmentation of the Golgi in response to decreased $PI(4,5)P_2$ synthesis might be attributed to the dissociation of βIII spectrin from Golgi membranes and concomitantly to its phosphorylation observed *in vitro* (21). We cannot rule out that βIII spectrin is subject to phosphorylation in Golgi membranes, but our antibodies and experimental conditions do not allow us to reach any conclusion concerning this question. Although some of the antibodies labeled two closely migrating bands in total cell lysates with the expected molecular weight of the protein, only the lower band was affected after silencing with the siRNAs. Therefore, the structural integrity of the Golgi architecture seems to be linked to a function of βIII spectrin related to phosphoinositide homeostasis, in which PI4P appears more relevant than $PI(4,5)P_2$.

The fragmentation of the Golgi complex as a result of the depletion of βIII spectrin is accompanied by a blockade in the protein transport of the integral membrane VSV-G and luminal proteins to the plasma membrane and the extracellular medium, respectively. We also observed a complete blockade of the Golgi reassembly during recovery from BFA and nocodazole treatments, consistent with a defect in the anterograde membrane flow from the ER. Such impairments could be linked to the reduced capacity to recruit dynein/dynactin motor complex in the absence of βIII spectrin. Under normal conditions, this motor complex mediates binding to Arp1 (29). Curiously, the dispersion of the fragments of the Golgi are not completely scattered throughout the cytoplasm but are restricted around the centrosome area, whose phenotype probably reflects the predominant unaffected activity of microtubule plus-end kinesin motor activity, which can be only partially compensated by the residual minus-end directed activity of βIII spectrin linked to the dynein/dynactin complex motor.

In conclusion, the use of new antibodies to human βIII spectrin unequivocally demonstrates its presence in the Golgi complex in a variety of mammalian cell lines and reveals its enrichment in distal compartments of the organelle. Moreover, knockdown experiments provided clear evidence for the importance of βIII spectrin in the maintenance of the structural integrity of the Golgi and in the anterograde secretory trafficking. Finally, PI4P is found to be a major determinant for the association of βIII spectrin to Golgi membranes.

Acknowledgments—We thank colleagues for generous gift of reagents and Maite Muñoz for technical support.

REFERENCES

1. Delaunay, J. (2007) The molecular basis of hereditary red cell membrane disorders. *Blood Rev.* **21,** 1–20
2. Bennett, V., and Healy, J. (2008) Organizing the fluid membrane bilayer: diseases linked to spectrin and ankyrin. *Trends Mol. Med.* **14,** 28–36
3. Machnicka, B., Grochowalska, R., Bogusławska, D. M., Sikorski, A. F., and Lecomte, M. C. (2012) Spectrin-based skeleton as an actor in cell signaling. *Cell Mol. Life Sci.* **69,** 191–201
4. Beck, K. A., Buchanan, J. A., Malhotra, V., and Nelson, W. J. (1994) Golgi spectrin: identification of an erythroid β-spectrin homolog associated with the Golgi complex. *J. Cell Biol.* **127,** 707–723
5. Bennett, V. (1989) The spectrin-actin junction of erythrocyte membrane skeletons. *Biochim. Biophys. Acta* **988,** 107–121
6. Bennett, V., and Baines, A. J. (2001) Spectrin and ankyrin-based pathways: metazoan inventions for integrating cells into tissues. *Physiol. Rev.* **81,** 1353–1392
7. Beck, K. A., and Nelson, W. J. (1998) A spectrin membrane skeleton of the Golgi complex. *Biochim. Biophys. Acta* **1404,** 153–160
8. Holleran, E. A., and Holzbaur, E. L. (1998) Speculating about spectrin: new insights into the Golgi-associated cytoskeleton. *Trends Cell Biol.* **8,** 26–29
9. De Matteis, M. A., and Morrow, J. S. (2000) Spectrin tethers and mesh in the biosynthetic pathway. *J. Cell Sci.* **113,** 2331–2343
10. De Matteis, M. A., and Morrow, J. S. (1998) The role of ankyrin and spectrin in membrane transport and domain formation. *Curr. Opin. Cell Biol.* **10,** 542–549
11. Holleran, E. A., Karki, S., and Holzbaur, E. L. (1998) The role of the dynactin complex in intracellular motility. *Int. Rev. Cytol.* **182,** 69–109
12. Stankewich, M. C., Tse, W. T., Peters, L. L., Ch'ng, Y., John, K. M., Stabach, P. R., Devarajan, P., Morrow, J. S., and Lux, S. E. (1998) A widely expressed βIII spectrin associated with Golgi and cytoplasmic vesicles. *Proc. Natl. Acad. Sci. U.S.A.* **95,** 14158–14163
13. Beck, K. A., Buchanan, J. A., and Nelson, W. J. (1997) Golgi membrane skeleton: identification, localization and oligomerization of a 195 kDa ankyrin isoform associated with the Golgi complex. *J. Cell Sci.* **110,** 1239–1249
14. Devarajan, P., Stabach, P. R., Mann, A. S., Ardito, T., Kashgarian, M., and Morrow, J. S. (1996) Identification of a small cytoplasmic ankyrin (AnkG119) in the kidney and muscle that binds βI sigma spectrin and associates with the Golgi apparatus. *J. Cell Biol.* **133,** 819–830
15. Kang, Q., Wang, T., Zhang, H., Mohandas, N., and An, X. (2009) A Golgi-associated protein 4.1B variant is required for assimilation of proteins in the membrane. *J. Cell Sci.* **122,** 1091–1099
16. Holappa, K., Muñoz, M. T., Egea, G., and Kellokumpu, S. (2004) The AE2 anion exchanger is necessary for the structural integrity of the Golgi apparatus in mammalian cells. *FEBS Lett.* **564,** 97–103
17. Percival, J. M., Hughes, J. A., Brown, D. L., Schevzov, G., Heimann, K., Vrhovski, B., Bryce, N., Stow, J. L., and Gunning, P. W. (2004) Targeting of a tropomyosin isoform to short microfilaments associated with the Golgi complex. *Mol. Biol. Cell* **15,** 268–280
18. Godi, A., Santone, I., Pertile, P., Devarajan, P., Stabach, P. R., Morrow, J. S., Di Tullio, G., Polishchuk, R., Petrucci, T. C., Luini, A., and De Matteis, M. A. (1998) ADP ribosylation factor regulates spectrin binding to the Golgi complex. *Proc. Natl. Acad. Sci. U.S.A.* **95,** 8607–8612
19. Godi, A., Pertile, P., Meyers, R., Marra, P., Di Tullio, G., Iurisci, C., Luini, A., Corda, D., and De Matteis, M. A. (1999) ARF mediates recruitment of PtdIns-4-OH kinase-β and stimulates synthesis of PtdIns(4,5)P2 on the Golgi complex. *Nat. Cell Biol.* **1,** 280–287
20. Muresan, V., Stankewich, M. C., Steffen, W., Morrow, J. S., Holzbaur, E. L., and Schnapp, B. J. (2001) Dynactin-dependent, dynein-driven vesicle transport in the absence of membrane proteins: a role for spectrin and

acidic phospholipids. *Mol. Cell* **7,** 173–183
21. Siddhanta, A., Radulescu, A., Stankewich, M. C., Morrow, J. S., and Shields, D. (2003) Fragmentation of the Golgi apparatus. A role for β III spectrin and synthesis of phosphatidylinositol 4,5-bisphosphate. *J. Biol. Chem.* **278,** 1957–1965
22. Devarajan, P., Stabach, P. R., De Matteis, M. A., and Morrow, J. S. (1997) Na,K-ATPase transport from endoplasmic reticulum to Golgi requires the Golgi spectrin-ankyrin G119 skeleton in Madin Darby canine kidney cells. *Proc. Natl. Acad. Sci. U.S.A.* **94,** 10711–10716
23. Ikeda, Y., Dick, K. A., Weatherspoon, M. R., Gincel, D., Armbrust, K. R., Dalton, J. C., Stevanin, G., Dürr, A., Zühlke, C., Bürk, K., Clark, H. B., Brice, A., Rothstein, J. D., Schut, L. J., Day, J. W., and Ranum, L. P. (2006) Spectrin mutations cause spinocerebellar ataxia type 5. *Nat. Genet.* **38,** 184–190
24. Clarkson, Y. L., Gillespie, T., Perkins, E. M., Lyndon, A. R., and Jackson, M. (2010) β-III spectrin mutation L253P associated with spinocerebellar ataxia type 5 interferes with binding to Arp1 and protein trafficking from the Golgi. *Hum. Mol. Genet.* **19,** 3634–3641
25. Perkins, E. M., Clarkson, Y. L., Sabatier, N., Longhurst, D. M., Millward, C. P., Jack, J., Toraiwa, J., Watanabe, M., Rothstein, J. D., Lyndon, A. R., Wyllie, D. J., Dutia, M. B., and Jackson, M. (2010) Loss of β-III spectrin leads to Purkinje cell dysfunction recapitulating the behavior and neuropathology of spinocerebellar ataxia type 5 in humans. *J. Neurosci.* **30,** 4857–4867
26. Stankewich, M. C., Gwynn, B., Ardito, T., Ji, L., Kim, J., Robledo, R. F., Lux, S. E., Peters, L. L., and Morrow, J. S. (2010) Targeted deletion of betaIII spectrin impairs synaptogenesis and generates ataxic and seizure phenotypes. *Proc. Natl. Acad. Sci. U.S.A.* **107,** 6022–6027
27. Lorenzo, D. N., Li, M. G., Mische, S. E., Armbrust, K. R., Ranum, L. P., and Hays, T. S. (2010) Spectrin mutations that cause spinocerebellar ataxia type 5 impair axonal transport and induce neurodegeneration in *Drosophila*. *J. Cell Biol.* **189,** 143–158
28. Watabe, H., Valencia, J. C., Le Pape, E., Yamaguchi, Y., Nakamura, M., Rouzaud, F., Hoashi, T., Kawa, Y., Mizoguchi, M., and Hearing, V. J. (2008) Involvement of dynein and spectrin with early melanosome transport and melanosomal protein trafficking. *J. Invest Dermatol.* **128,** 162–174
29. Holleran, E. A., Ligon, L. A., Tokito, M., Stankewich, M. C., Morrow, J. S., and Holzbaur, E. L. (2001) β III spectrin binds to the Arp1 subunit of dynactin. *J. Biol. Chem.* **276,** 36598–36605
30. Johansson, M., Rocha, N., Zwart, W., Jordens, I., Janssen, L., Kuijl, C., Olkkonen, V. M., and Neefjes, J. (2007) Activation of endosomal dynein motors by stepwise assembly of Rab7-RILP-p150Glued, ORP1L, and the receptor βlll spectrin. *J. Cell Biol.* **176,** 459–471
31. Bard, F., Mazelin, L., Péchoux-Longin, C., Malhotra, V., and Jurdic, P. (2003) Src regulates Golgi structure and KDEL receptor-dependent retrograde transport to the endoplasmic reticulum. *J. Biol. Chem.* **278,** 46601–46606
32. Hui, N., Nakamura, N., Slusarewicz, P., and Warren, G. (1998) *Cell Biology: A Laboratory Handbook*, 2nd Ed., Vol. 2, Academic Press, Inc., NY
33. Szentpetery, Z., Várnai, P., and Balla, T. (2010) Acute manipulation of Golgi phosphoinositides to assess their importance in cellular trafficking and signaling. *Proc. Natl. Acad. Sci. U.S.A.* **107,** 8225–8230
34. Johannes, L., Tenza, D., Antony, C., and Goud, B. (1997) Retrograde transport of KDEL-bearing B-fragment of Shiga toxin. *J. Biol. Chem.* **272,** 19554–19561
35. Harlan, J. E., Hajduk, P. J., Yoon, H. S., and Fesik, S. W. (1994) Pleckstrin homology domains bind to phosphatidylinositol-4,5-bisphosphate. *Nature* **371,** 168–170
36. Hyvönen, M., Macias, M. J., Nilges, M., Oschkinat, H., Saraste, M., and Wilmanns, M. (1995) Structure of the binding site for inositol phosphates in a PH domain. *EMBO J.* **14,** 4676–4685
37. Lemmon, M. A., Ferguson, K. M., and Abrams, C. S. (2002) Pleckstrin homology domains and the cytoskeleton. *FEBS Lett.* **513,** 71–76
38. De Matteis, M. A., Di Campli, A., and Godi, A. (2005) The role of the phosphoinositides at the Golgi complex. *Biochim. Biophys. Acta* **1744,** 396–405
39. D'Angelo, G., Vicinanza, M., Wilson, C., and De Matteis, M. A. (2012) Phosphoinositides in Golgi complex function. *Subcell. Biochem.* **59,** 255–270
40. Levine, T. P., and Munro, S. (2002) Targeting of Golgi-specific pleckstrin homology domains involves both PtdIns 4-kinase-dependent and -independent components. *Curr. Biol.* **12,** 695–704
41. Dowler, S., Currie, R. A., Campbell, D. G., Deak, M., Kular, G., Downes, C. P., and Alessi, D. R. (2000) Identification of pleckstrin-homology-domain-containing proteins with novel phosphoinositide-binding specificities. *Biochem. J.* **351,** 19–31
42. Colón-Franco, J. M., Gomez, T. S., and Billadeau, D. D. (2011) Dynamic remodeling of the actin cytoskeleton by FMNL1γ is required for structural maintenance of the Golgi complex. *J. Cell Sci.* **124,** 3118–3126
43. Képès, F., Rambourg, A., and Satiat-Jeunemaître, B. (2005) Morphodynamics of the secretory pathway. *Int. Rev. Cytol.* **242,** 55–120
44. De Matteis, M. A., and Luini, A. (2008) Exiting the Golgi complex. *Nat. Rev. Mol. Cell Biol.* **9,** 273–284
45. Graham, T. R., and Burd, C. G. (2011) Coordination of Golgi functions by phosphatidylinositol 4-kinases. *Trends Cell Biol.* **21,** 113–121
46. Dippold, H. C., Ng, M. M., Farber-Katz, S. E., Lee, S. K., Kerr, M. L., Peterman, M. C., Sim, R., Wiharto, P. A., Galbraith, K. A., Madhavarapu, S., Fuchs, G. J., Meerloo, T., Farquhar, M. G., Zhou, H., and Field, S. J. (2009) GOLPH3 bridges phosphatidylinositol-4- phosphate and actomyosin to stretch and shape the Golgi to promote budding. *Cell* **139,** 337–351
47. Wood, C. S., Schmitz, K. R., Bessman, N. J., Setty, T. G., Ferguson, K. M., and Burd, C. G. (2009) PtdIns4P recognition by Vps74/GOLPH3 links PtdIns 4-kinase signaling to retrograde Golgi trafficking. *J. Cell Biol.* **187,** 967–975
48. Mizuno-Yamasaki, E., Medkova, M., Coleman, J., and Novick, P. (2010) Phosphatidylinositol 4-phosphate controls both membrane recruitment and a regulatory switch of the Rab GEF Sec2p. *Dev. Cell* **18,** 828–840